

Highlights

Space Syntax-guided Post-training for Residential Floor Plan Generation

Zhuoyang Jiang, Dongqing Zhang

- SSPT: space syntax-guided post-training for diffusion-based floor plan generation.
- A rectangle-space oracle computes integration and public-space dominance at scale.
- SSPT-Bench (Eval-8) enables unified, reproducible evaluation under OOD constraints.
- PPO post-training improves dominance and stability with $> 10\times$ efficiency.

Space Syntax-guided Post-training for Residential Floor Plan Generation [★]

Zhuoyang Jiang^{a,b,1}, Dongqing Zhang^{a,*}

^aCollege of Architecture and Urban Planning, Tongji University, Shanghai, China

^bInformation Hub, The Hong Kong University of Science and Technology (Guangzhou), Guangzhou, China

ARTICLE INFO

Keywords:

Residential floor plan generation
Space syntax
Post-training
Iterative retraining
Proximal policy optimization (PPO)
Evaluation benchmark

ABSTRACT

Pre-trained generative models for residential floor plans are typically optimized to fit large-scale data distributions, which can under-emphasize critical architectural priors such as the configurational dominance and connectivity of domestic public spaces (e.g., living rooms and foyers). This paper proposes **Space Syntax-guided Post-training (SSPT)**, a post-training paradigm that explicitly injects space syntax knowledge into floor plan generation via a non-differentiable oracle. The oracle converts RPLAN-style layouts into rectangle-space graphs through greedy maximal-rectangle decomposition and door-mediated adjacency construction, and then computes integration-based measurements to quantify public space dominance and functional hierarchy.

To enable consistent evaluation and diagnosis, we further introduce **SSPT-Bench (Eval-8)**, an out-of-distribution benchmark that post-trains models using conditions capped at ≤ 7 rooms while evaluating on 8-room programs, together with a unified metric suite for dominance, stability, and profile alignment. SSPT is instantiated with two strategies: (i) *iterative retraining* via space-syntax filtering and diffusion fine-tuning, and (ii) *reinforcement learning* via PPO with space-syntax rewards. Experiments show that both strategies improve public-space dominance and restore clearer functional hierarchy compared to distribution-fitted baselines, while PPO achieves stronger gains with substantially higher compute efficiency and reduced variance. SSPT provides a scalable pathway for integrating architectural theory into data-driven plan generation and is compatible with other generative backbones given a post-hoc evaluation oracle.

1. Introduction

Recent advances in artificial intelligence (AI) have led to rapid progress in the automated generation of residential floor plans. Deep learning-based approaches, including generative adversarial networks, diffusion models, and graph-based generative methods, are increasingly capable of producing large numbers of layout candidates with minimal human intervention. These developments hold significant promise for improving design efficiency and supporting early-stage architectural exploration. However, the growing quantity of generated layouts has also exposed a fundamental challenge: how to systematically evaluate the architectural rationality and spatial quality of residential floor plans at scale.

Existing evaluation approaches for residential layouts largely rely on geometric constraints, adjacency rules, or manually defined heuristics, such as room size compliance, functional adjacency matrices, or circulation completeness. While these criteria are useful for ensuring basic feasibility, they often fail to capture deeper spatial properties that are central to architectural design logic, particularly the role of spatial centrality, accessibility, and hierarchical organization of domestic space. As a result, many automatically generated floor plans may satisfy formal constraints while still exhibiting spatial configurations that contradict long-established

architectural principles, such as the central role of public living zones or the clear differentiation between public and private zones. In accordance with established architectural principles, "public spaces" within a domestic layout (primarily living rooms and foyers) are characterized by their superior openness and collective accessibility, serving as the topological integrators of the plan. This distinguishes them from "private quarters" (such as bedrooms and bathrooms) which, by design, prioritize enclosure and seclusion. We employ the term "public" to reflect this inherent functional hierarchy and structural centrality. By measuring global integration and mean depth, we can objectively evaluate whether a generated plan maintains the high-connectivity core that is essential for a functionally coherent and habitable home.

A related but less discussed issue concerns the quality of large-scale residential floor plan datasets that are commonly used for both empirical studies and AI model training. Widely adopted datasets, such as RPLAN, CubiCasa, and similar repositories, contain tens of thousands of real-world housing layouts. These datasets are typically treated as reliable ground truth representations of architectural practice. However, due to heterogeneous sources, automated annotation, and varying design standards, they may include layouts with problematic spatial logic, mislabelled functions, or atypical configurations. At present, there is no established automated method to systematically screen such datasets for spatial rationality prior to analysis or model training, and manual inspection is infeasible at scale.

*

*Corresponding author

✉ zhangdongqing@tongji.edu.cn (D. Zhang)

ORCID(s):

¹These authors contributed equally.

Space syntax theory offers a well-established conceptual and analytical framework for understanding spatial configuration and human movement patterns in architectural and urban environments. Among its core metrics, spatial integration has been widely used to describe how centrally a space is embedded within a spatial system, reflecting its accessibility and potential to attract movement. In residential architecture, decades of empirical and theoretical research have consistently emphasized that public activity spaces—such as living rooms and dining areas—tend to function as integration cores, while private spaces such as bedrooms and bathrooms occupy more segregated positions. Despite its strong theoretical relevance, spatial integration has rarely been operationalized as an automated, large-scale evaluation tool for residential floor plans, and its application has largely been confined to small-sample or case-based studies.

This study argues that spatial integration can serve not only as an analytical descriptor but also as a computational criterion for automated screening and evaluation of residential floor plans. By translating architectural design knowledge into measurable, scalable indicators, integration-based analysis has the potential to bridge the gap between architectural theory and AI-driven design workflows. Specifically, integration values can be used to identify spatial configurations that violate fundamental residential design logic, extract empirical spatial patterns from large datasets, and provide objective benchmarks for evaluating AI-generated layouts.

To this end, this paper proposes an integration-based framework for automated screening and evaluation of residential floor plans. The framework combines three key methodological components. First, spatial integration metrics derived from space syntax theory are computed automatically from room-level connectivity graphs, enabling batch processing of large numbers of floor plans. Second, a large-scale dataset analysis is conducted using over 80,000 real residential layouts from the RPLAN dataset, allowing empirical distributions of integration values across different functional spaces to be statistically examined. Third, the derived empirical integration patterns are used as a reference system to evaluate AI-generated residential floor plans, assessing whether their spatial configurations conform to or deviate from observed architectural norms.

The proposed framework supports three complementary analytical objectives. First, it enables the automated identification and removal of unreasonable or problematic floor plans within large real-world datasets, without reliance on manual inspection. Layouts in which public spaces fail to exhibit integration dominance, or in which circulation spaces become anomalously central, can be efficiently detected as potential errors or atypical cases. Second, it facilitates the extraction of large-scale empirical architectural knowledge by quantifying integration patterns of different functional spaces across thousands of real residential layouts. The analysis confirms that living rooms consistently exhibit the

highest integration values, followed by other public or semi-public areas, providing quantitative evidence for long-held architectural design principles based on extensive real-world data. Third, the framework enables systematic evaluation of AI-generated residential layouts by comparing their integration profiles with empirical benchmarks derived from real housing, thereby revealing common biases, limitations, and strengths of current generative models.

The main contributions of this study are fourfold.

- (1) **Architectural prior:** We introduce space syntax integration as a computable architectural prior for residential floorplan generation, formalizing the public-space dominance principle as a theory-grounded target for evaluation and optimization.
- (2) **Data/representation:** We design a mask-to-graph representation and an automated rectangle-based convex-integration oracle that reliably converts RPLAN-style layouts into a rectangle-space graph and computes integration-based measurements at scale, enabling dataset screening and empirical knowledge extraction.
- (3) **Task/benchmark:** We construct a unified evaluation benchmark (SSPT-Bench / Eval-8) and a corresponding metric suite that quantifies public-space dominance and functional-hierarchy alignment, supporting consistent and reproducible assessment of prior-guided generation.
- (4) **Model/post-training:** We propose SSPT, a space-syntax-guided post-training framework for diffusion-based floorplan generators, and instantiate two post-training paradigms (SSPT-Iter and SSPT-PPO) with practical training configurations; experiments demonstrate improved architectural alignment and substantially higher compute efficiency.

By demonstrating how spatial integration can be operationalized as an automated and scalable evaluation criterion, this research contributes to the growing field of AI-assisted architectural design and construction informatics. The proposed framework not only enhances the reliability of large residential datasets but also provides a meaningful pathway for integrating architectural theory into the evaluation and future optimization of AI-generated design outcomes.

2. Literature Review

2.1. Interdisciplinary Task Formulations for Generative Residential Layouts

2.1.1. Formal Task Definition and Complexity

In the domain of computational design, residential floor plan generation is formulated as a constrained spatial partitioning problem within a non-convex domain [46]. Formally, given a set of input constraints C , encompassing geometric boundary conditions C_g (e.g., site contours, structural envelopes) and functional semantic requirements C_s (e.g., room programs and topological adjacency graphs), the objective is to learn a generative mapping that produces spatially-coherent layout configurations. This task is characterized by high-dimensional complexity and discrete-continuous hybridity[29]: while room labels are discrete,

their boundary coordinates are continuous, and the entire system must satisfy Euler’s characteristic for planar partitions. Unlike generic image synthesis, this task necessitates a high degree of topological fidelity[47], requiring models to navigate a vast search space to satisfy both hard physical constraints (e.g., non-overlapping partitioning) and soft performance objectives (e.g., natural light accessibility). Consequently, the field has evolved from early rule-based heuristic search into a probabilistic distribution modeling problem, where the core challenge lies in aligning the stochastic output of deep generative models with the rigorous, non-differentiable requirements of human-centric design[44].

2.1.2. Methodological Evolution of AI-based Floorplan Generation

The technical trajectory of automated floorplan generation has transitioned from early heuristic pipelines to deep generative paradigms that learn distributional priors from large datasets. Existing methods can be grouped by their dominant representation and backbone:

- **Rasterized mask generation (CNNs / GANs):** Early learning-based systems rasterize plans into multi-channel images and predict room/wall masks from boundary cues using CNNs (e.g., RPLAN) [46]. Subsequent variants incorporate adversarial learning or human-in-the-loop corrections to improve realism and controllability [15, 24].
- **Graph-conditioned generation (GNNs / graph Transformers):** To explicitly encode architectural semantics, many methods condition generation on bubble diagrams or adjacency graphs, and use GNNs or relational GANs to enforce graph constraints during synthesis [18, 29]. Extensions such as HouseGAN++ add stronger supervision and test-time optimization to refine graph compatibility [30]. More recent works explore graph Transformers and hybrid optimization for constraint-aware generation under bubble-diagram constraints [1, 42, 43, 51].
- **Vectorized sequence generation (Transformers):** Beyond raster grids, vectorized representations model a plan as coordinate sequences or structural graphs (e.g., wall graphs), enabling higher geometric precision and easier downstream CAD use. Autoregressive Transformers have been used to generate vectorized layouts conditioned on constraint graphs, often coupled with refinement modules for panoptic or geometric consistency [23, 32, 41].
- **Diffusion-based generation:** Diffusion models further improve diversity and geometric fidelity by iteratively denoising vectorized layouts. HouseDiffusion demonstrates conditional diffusion for polygonal (including non-Manhattan) floorplans, and follow-up work integrates geometry-aware graph diffusion to better capture structural constraints [19, 39].

2.1.3. Data Foundations and Benchmarking

The efficacy of generative models is fundamentally constrained by the semantic richness and scale of the training data.

Regional and Scale Taxonomy Most learning-based studies focus on the *unit* scale, where the task is conditioned on boundary/program constraints and outputs a single dwelling layout. Representative large-scale unit datasets include RPLAN (80k+ densely annotated residential layouts) [46] and LI-FULL HOME (millions of real floor plans, enabling scalable bubble-diagram extraction) [22]. Beyond 2D plans, dataset design has expanded toward richer modalities and downstream use cases: Structured3D provides paired floor plans and structured 3D scene data [50], ZInD offers large-scale real indoor panoramas with both Manhattan and non-Manhattan layouts [8], and CubiCasa5K provides object-level furniture annotations for fine-grained indoor layout understanding [21]. Recent efforts also connect floorplan generation to embodied and language-conditioned settings, such as ProcTHOR-10k for procedurally generated embodied environments [9] and DStruct2Design for language-friendly structured representations built from multiple sources [25].

Modality and Evaluation Metrics Modern datasets and models have evolved from simple raster masks to hybrid representations (raster + graph + vector), which enables stronger conditioning interfaces (e.g., bubble graphs), higher-precision outputs (vector polygons), and broader multimodal supervision (3D, object instances, language). Correspondingly, evaluation metrics have shifted from visual realism (e.g., FID) and geometric accuracy (e.g., IoU) to topology-aware criteria (e.g., graph edit distance or constraint satisfaction on adjacency graphs). However, as summarized in Table 1, most benchmarks still under-emphasize the *configurational logic* of domestic space (e.g., hierarchy and accessibility patterns). This motivates the introduction of performance-oriented evaluation mechanisms grounded in architectural theory—in our case, Space Syntax—to bridge the gap between stochastic generation and rigorous spatial logic.

2.2. Architectural Criteria and Spatial Logic for Plan Assessment

2.2.1. Evaluation and Quality Assessment of Floor Plans

Several studies have attempted to formalize evaluation criteria for residential floor plans by introducing multi-objective scoring systems or rule-based assessment models[7]. These approaches typically combine indicators related to room area compliance, functional adjacency satisfaction, circulation efficiency, and sometimes daylight or ventilation proxies[46]. Such frameworks are often used either to rank generated layouts or to guide optimization during generation[32].

However, two major limitations can be identified. First, many evaluation criteria are highly context-dependent and rely on manually defined weights or expert-defined thresholds[35],

Table 1
Summary of representative datasets in floorplan generation.

Dataset	Scale	Key Features	Primary Task
RPLAN [46]	80k+	Vectorized, densely annotated floor plans	Residential unit generation
LIFULL HOME [22]	Millions	Real-world plans; bubble extraction at scale	Data foundation / layout study
ZInD [8]	70k+ pano / 2.5k+ scenes	Real indoor data; Manhattan + non-Manhattan	Geometry-aware indoor modeling
CubiCasa5K [21]	5k	Furniture/object-level annotations	Fine-grained interior understanding
Structured3D [50]	3.5k+	Structured 3D scenes with floorplan meta-data	Multi-modal scene synthesis
ProcTHOR-10k [9]	10k	Procedural embodied environments with objects	Embodied AI / procedural layouts
DStruct2Design [25]	Multi-source	Language-friendly structured representations	Language-guided generation

limiting their generalizability and scalability. Second, most existing evaluation frameworks treat different indicators as compensatory, allowing poor performance in one aspect to be offset by better performance in another[44]. In architectural practice, however, certain spatial principles—such as the central role of public spaces in cities[5] and living room in houses[34]—function as non-compensatory requirements, and their violation cannot be easily justified by improvements elsewhere.

Moreover, evaluation methods are rarely validated against large-scale empirical evidence from real residential layouts. As a result, it remains unclear whether the adopted evaluation criteria reflect common architectural practice or merely encode designer preferences.

2.2.2. Space Syntax as a Computational Prior for Functional Alignment

Space syntax theory provides a well-established framework for analyzing spatial configuration and its relationship to movement[17][2], accessibility, and social interaction[4]. Among its core measures, spatial integration quantifies how centrally a space is embedded within a spatial system by considering its topological or metric distance to all other spaces[20]. Higher integration values indicate greater accessibility and a higher potential to attract movement[26].

In residential architecture, space syntax has been used to examine spatial hierarchies[11], circulation patterns, and the relationship between public and private spaces. Numerous case-based studies have demonstrated that living rooms and other shared spaces tend to occupy integrated positions, while bedrooms and service spaces are more segregated[14][10]. These findings align with long-standing architectural design knowledge regarding domestic spatial organization.

Nevertheless, the application of space syntax in residential studies has largely been limited to small samples or individual case analyses due to the effort required for manual modeling and interpretation[3]. Although recent studies have begun to explore automated or semi-automated syntax

computation[16], the use of integration metrics as a large-scale, batch-processing evaluation tool for residential floor plans remains underexplored. In particular, integration has rarely been employed as a criterion for automated screening or quality control in large datasets or AI-generated design outputs.

2.3. Advanced AI Paradigms for Knowledge-Guided Generative Design

Cross-disciplinary generative tasks increasingly require models to satisfy explicit constraints and domain knowledge that are difficult to capture via standard maximum-likelihood pre-training alone. Recent advances in generative AI suggest multiple practical pathways for injecting such knowledge into a generator, especially when supervision is sparse, non-differentiable, or preference-based.

2.3.1. Knowledge-guided Generation Systems

We summarize representative knowledge-guided generation mechanisms into four categories that are broadly applicable across design domains:

(1) *Conditional generation.* A direct way to encode knowledge is to expose it as *conditions* that steer the generator (e.g., boundary constraints, program requirements, or structured graphs). Conditional generative frameworks, such as conditional GANs [27], and more recent conditioning architectures for diffusion models (e.g., ControlNet-style spatial controls) [48], demonstrate that explicit control signals can substantially improve controllability without requiring hand-crafted post-processing rules.

(2) *Evolutionary algorithms and black-box optimization.* When constraints are non-differentiable or only accessible through an oracle, evolutionary strategies provide a general-purpose optimization route by treating the generator (or its latent variables) as a search space. Classical approaches such as CMA-ES [13] and quality-diversity methods such as MAP-Elites [28] are attractive for design settings

because they naturally handle discrete constraints, multi-objective trade-offs, and diversity-seeking exploration.

(3) *Iterative retraining (generate–filter–retrain)*. Another scalable mechanism is to iteratively generate candidates, filter them using an oracle/critic, and retrain the model on the curated subset. This “dataset aggregation” pattern has strong precedents in sequential learning (e.g., DAgger) [37], and has been widely adopted in modern foundation-model post-training pipelines where model generations are filtered and recycled as training data [40, 45]. In our problem setting, this mechanism is particularly appealing because architectural validity and configurational quality can be assessed post-hoc by deterministic analysis tools.

(4) *Reinforcement learning*. Reinforcement learning (RL) treats the generator as a stochastic policy and directly optimizes an expected reward that can encode domain knowledge, preferences, and hard penalties. Policy-gradient methods such as PPO [38] have become a standard post-training tool for aligning large language models with human feedback [31]. Similar ideas have recently been explored for aligning diffusion models using learned reward functions [12], indicating that RL-style post-training can serve as a general recipe for optimizing non-differentiable objectives in generation.

2.3.2. Pre-training and Post-training Paradigms

The prevailing paradigm in modern AI is to first pre-train large generative models for broad distribution learning, and then apply *post-training* to specialize, align, and constrain the model for a target domain.

(1) *Post-training for alignment and controllability*. In foundation models, post-training has emerged as a critical step to improve instruction following, preference alignment, and safety, typically through a combination of supervised fine-tuning and preference-based optimization [6, 31, 33]. This highlights a key insight: distribution fitting alone may not yield behavior that satisfies user intent or domain desiderata, motivating explicit post-hoc alignment objectives.

(2) *Generative processes as MDPs for reinforcement learning*. Many generators can be naturally formulated as finite-horizon Markov decision processes (MDPs): LLMs generate tokens sequentially (actions), and diffusion models generate samples via multi-step denoising trajectories. This view enables policy optimization on intermediate transitions while only receiving terminal rewards from an oracle. Recent work has formalized RL fine-tuning for diffusion models by defining the denoising process as an RL problem and optimizing with policy gradients and KL-regularized objectives [12, 49]. In robotics, related policy-gradient frameworks have also been proposed to fine-tune diffusion-based policies by explicitly treating denoising steps as an optimizable decision process [36].

These advances collectively motivate our SSPT design: we retain the strong geometric prior learned by pre-training, while using a deterministic space-syntax oracle to enable knowledge-guided post-training through both iterative retraining and PPO-based reinforcement learning.

2.4. Research Gap

Despite rapid progress in representation learning and generative backbones (Sec. 2.1) and the growing interest in architectural evaluation criteria (Sec. 2.2), several gaps remain that limit both the *reliability* and *architectural alignment* of AI-generated residential layouts.

Gap 1: Metrics and benchmarks under-emphasize configurational logic. Most large-scale evaluation pipelines emphasize geometric feasibility, mask/polygon similarity, or local adjacency satisfaction, while the deeper configurational hierarchy of domestic space—how accessibility and centrality distribute across functional zones—is rarely enforced as a first-class objective. Although space syntax provides theory-grounded measures such as integration, it is not yet commonly operationalized as a scalable oracle that can evaluate (and supervise) generative outputs in batch.

Gap 2: Knowledge is rarely injected through systematic post-training. As reviewed in Sec. 2.3, modern foundation models increasingly rely on post-training (e.g., generate–filter–retrain loops and RL-based alignment) to satisfy non-differentiable objectives and preference-style constraints [6, 12, 31]. In contrast, most residential floorplan generators are still optimized primarily during pre-training to fit the training distribution, leaving critical architectural priors to be captured only implicitly and often weakly.

Gap 3: Lack of unified protocols for diagnosis and OOD evaluation. Even when a generative model achieves strong in-distribution geometric fidelity, it remains unclear whether it robustly preserves functional hierarchy under distribution shift (e.g., novel program sizes or atypical constraint combinations). The field lacks a unified benchmark protocol and a consistent metric suite that can (i) diagnose failure modes in public/private hierarchy and (ii) quantify improvements attributable to prior-guided post-training.

Our motivation: These gaps call for a reproducible, theory-grounded evaluation oracle and a practical post-training framework that can *explicitly* reinforce architectural priors. This motivates our SSPT framework: a deterministic space-syntax oracle that computes integration-based dominance and profile metrics at scale, together with two complementary post-training strategies—iterative retraining via oracle-based filtering and reinforcement learning via PPO—evaluated under a unified out-of-distribution benchmark.

3. Methodology

Based on the design of the data foundation and the benchmark, we propose two distinct post-training paradigms

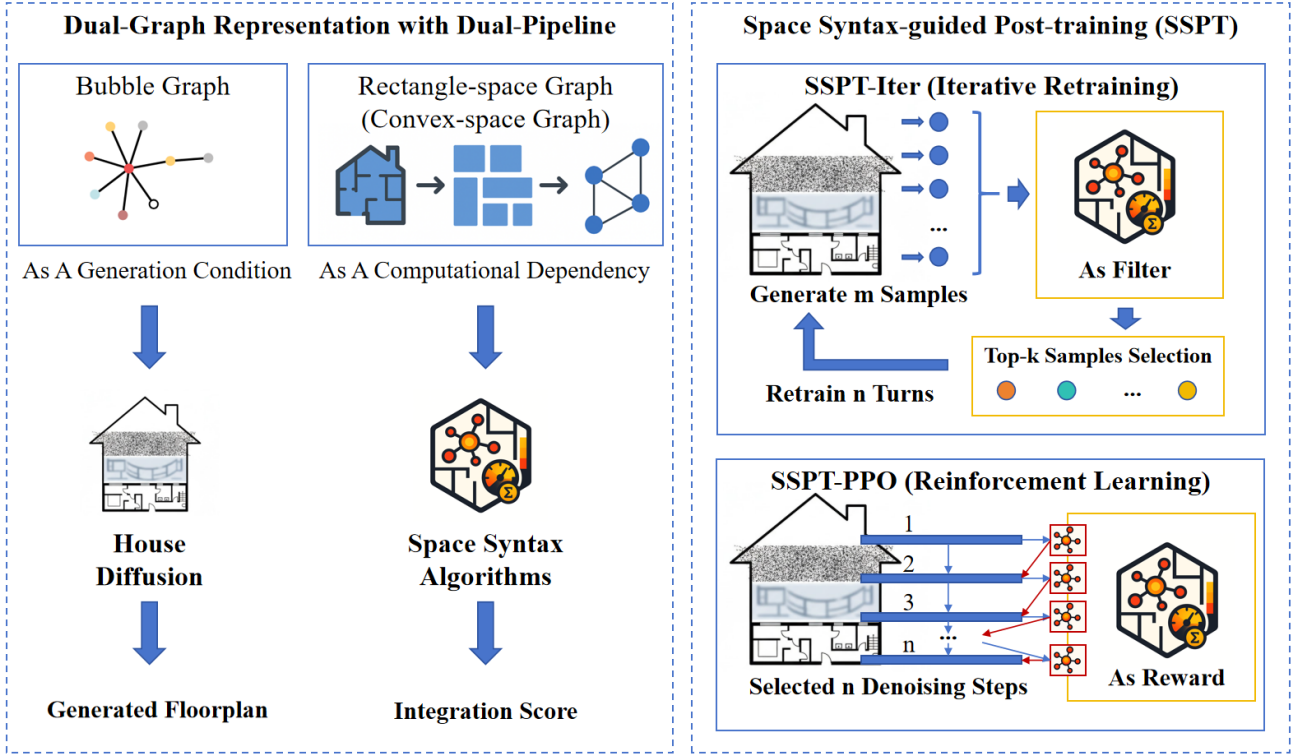


Figure 1: Overview Framework

to bridge the gap between generative probability and spatial logic. The overview framework is in Figure 1.

3.1. Data Foundation: Representation Learning and Space Syntax Algorithms

3.1.1. Dual-Graph Representation and Spatial Abstraction

To bridge the gap between pixel-level floorplan representations and graph-based configurational analysis, we adopt a deterministic *mask-to-graph* abstraction that is compatible with the RPLAN data format and our generative pipeline. Concretely, each layout is represented as a 4-channel PNG encoding: (i) boundary/door cues, (ii) semantic function labels, (iii) room instance ids, and (iv) interior/exterior region flags. From these channels we derive three binary masks that are essential for accessibility modeling: an interior mask, a wall mask, and a door mask. For each room instance r (instance id > 0), we extract its *walkable core* by removing wall and door pixels from the interior region.

To obtain a compact yet robust spatial partition without fragile polygon extraction, we decompose each room core mask into a set of maximal axis-aligned rectangles using a greedy covering algorithm with a minimum rectangle area threshold A_{\min} . Each rectangle serves as a convex *spatial atom* (node). The union of rectangles across all rooms forms a *rectangle-space graph* $G = (V, E)$, where nodes inherit room-instance and semantic type attributes. Edges are constructed in two complementary ways: (i) *within-room* edges

connect rectangles that touch or lie within a small pixel-distance, with additional bridging edges inserted between disconnected components to ensure intra-room connectivity; and (ii) *cross-room* edges are induced by interior-door connected components, which provide reliable evidence of accessibility between room instances. This representation preserves the key topological structure required by space syntax while enabling scalable and reproducible batch computation.

3.1.2. Automated Integration Computation and Quality-Check Oracle

To enable automated and scalable analysis of residential floor plans, architectural layouts are abstracted from continuous geometric space into discrete topological representations. Following space syntax principles, spatial relationships are modeled by retaining only adjacency and accessibility between spaces, while metric information is omitted, allowing spatial configurations to be analyzed in a consistent and computationally efficient manner. In our implementation, each residential layout is decomposed into rectangle-based convex atoms (Sec. 3.1.1) that form a rectangle-space graph $G = (V, E)$, where edges represent direct accessibility cues induced by same-room proximity and door-mediated cross-room connections.

Spatial integration is computed based on depth relationships on G . For a given node i , the total depth TD_i is the sum of shortest-path distances to all other nodes. Mean depth

MD_i is defined as:

$$MD_i = \frac{TD_i}{k-1}, \quad (1)$$

where $k = |V|$ denotes the number of nodes in the spatial graph. To normalize across layouts of different sizes, relative asymmetry (RA) is computed as:

$$RA_i = \frac{2(MD_i - 1)}{k - 2}. \quad (2)$$

The final spatial integration is obtained by standardizing and inverting RA , resulting in a positively correlated indicator of spatial centrality:

$$Integration_i = \frac{1}{RRA_i}. \quad (3)$$

Higher values indicate spaces that are topologically closer to all others and thus more likely to function as configurational cores.

The integration values provide a direct basis for an automated screening oracle that enforces the fundamental architectural principle that public space should function as spatial cores. The oracle is implemented as a deterministic, non-compensatory pipeline consisting of five stages:

1. **Mask parsing and derived masks.** RPLAN-style 4-channel layout masks are parsed to obtain semantic labels, room instances, and interior/exterior flags. Interior, wall, and door masks are derived deterministically from the channels for subsequent accessibility analysis.
2. **Rectangle decomposition (greedy maximal cover).** For each room instance, its walkable core is decomposed into a set of maximal axis-aligned rectangles using greedy covering, discarding rectangles whose area is below a minimum threshold A_{\min} .
3. **Rectangle-space graph construction.** Each rectangle becomes a node. Within-room edges connect rectangles that touch or lie within a small pixel-distance, and additional bridge edges are inserted to enforce intra-room connectivity. Cross-room edges are determined by interior-door connected components, which yield reliable room-to-room accessibility pairs; for each adjacent room pair, the nearest rectangle pair is connected.
4. **Integration computation and room-instance aggregation.** Global integration is computed per node on G (HH or closeness). Node scores are aggregated to room-instance mean integration by averaging over the rectangles belonging to that room instance:

$$\bar{s}_r = \frac{1}{|V_r|} \sum_{v \in V_r} s_v, \quad (4)$$

where V_r is the set of rectangle nodes for room instance r .

5. **Validity checks and scoring hooks.** Invalid samples (e.g., empty cores or zero extracted rectangles) are skipped during batch processing. For SSPT post-training, we additionally apply non-compensatory validity gates and penalties derived from oracle outputs (e.g., missing living room, too few rooms, abnormal living-room area share), and we use the same score definition for both iterative filtering and PPO reward construction (Sec. 3.4.2–3.4.3).

By transforming semantic masks into graphs that admit exact, reproducible measurements, the oracle flags layouts where public spaces lack centrality or where threshold/circulation spaces (e.g., Entrance) become anomalously central. These screening rules function as strict constraints, ensuring that only plans with valid functional logic are used for subsequent statistical analysis or AI model optimization.

3.2. Preliminary Experiment: Empirical Discovery on Representative Datasets and Baselines

3.2.1. Analysis of Representative Datasets and Data Selection

Using the screened RPLAN dataset, integration values were aggregated and normalized within each floor plan to enable cross-layout comparison. Fig. 2 presents the overall relative integration patterns across different room types, showing median values and interquartile ranges. The results reveal a clear and consistent spatial hierarchy. Living rooms exhibit the highest relative integration, with a median value significantly above the per-plan average (normalized to 1), indicating that they function as the primary spatial cores in the vast majority of residential layouts. Dining rooms rank second, with median integration values slightly above the average, reflecting their frequent role as semi-public connectors between living areas and other functional spaces.

In contrast, private spaces such as bedrooms, study rooms, and child rooms display lower relative integration values, generally clustering below the normalized average. Service spaces—including kitchens, bathrooms, storage rooms, and walk-in closets—are even more segregated, indicating limited spatial centrality and reduced movement potential. Balconies exhibit the lowest integration values overall, consistent with their peripheral and often externally oriented spatial roles. Entrance spaces show moderate integration levels with relatively wide variability, reflecting different layout strategies in which entrances may function either as transitional connectors or as relatively isolated access points depending on design typology. Overall, the consistent separation between public and private spaces in terms of integration values provides large-scale empirical validation of common residential layout practice: spaces intended for shared activities tend to occupy more central and accessible positions, while private and service spaces are typically arranged in more segregated locations to support functional separation and privacy. Importantly, this conclusion is derived from quantitative evidence over tens of thousands of real residential layouts, transforming

qualitative design intuition into measurable architectural benchmarks.

To reduce potential single-dataset bias, we further examined whether the observed integration hierarchy can be reproduced in an additional widely used dataset, LIFULL (Japan), which contains 145,811 annotated residential layouts. Compared with RPLAN (China), LIFULL reflects different housing typologies and labeling practices, leading to region-specific discrepancies in room-type coverage and semantic definition (Fig. 3a). First, Japanese housing frequently follows an “entrance (Genkan) → corridor → rooms” organization in which entrance and circulation are explicit spatial units; thus, a substantial amount of shared transition space is annotated as corridor/entrance (or occasionally other/missing) rather than as living room, making these labels more prominent and higher-coverage. Second, functional mixing is common due to the LDK pattern (Living–Dining–Kitchen integration), where a unified public space may be annotated as kitchen or dining room rather than as a distinct living room. Third, smaller unit typologies (e.g., 1R/1K/1DK/1LDK) often embed “living” functions within a multi-purpose room labeled as bedroom, further shifting room-type statistics. These differences can directly influence fine-grained room-type integration curves and complicate one-to-one comparisons of room labels across datasets.

To enable a robust cross-dataset comparison, we mapped room types from both datasets into higher-level functional domains and compared domain-level relative integration patterns (Fig. 3b). The domain mapping includes: Public/Communal (Living + Dining; optionally including corridor when it primarily serves shared transition), Private (Bedrooms), Service/Wet (Kitchen + Bathroom + Laundry), Circulation/Threshold (Entrance + Corridor), Storage/Utility (Storage + Closet/Walk-in), and Outdoor/Semi-outdoor (Balcony). Despite typological and annotation differences, Fig. 3b shows a consistent domain-level hierarchy across RPLAN and LIFULL: public/communal domains exhibit the highest relative integration, whereas private, service, outdoor, and storage-related domains are generally less integrated. This cross-dataset consistency provides additional empirical support that “public space dominance” in integration is not merely an artifact of a single dataset but reflects a reproducible configurational property in residential layouts.

In the remainder of this study, we adopt RPLAN as the primary empirical benchmark for model development and evaluation because it offers large-scale, consistently annotated room categories that enable standardized comparisons across model families and pipelines. Many representative learning-based residential layout generation studies have evaluated on RPLAN-derived benchmarks (e.g., Graph2Plan; House-GAN; House-GAN++), making it a practical reference for situating new models and evaluation criteria within the existing research landscape. Nevertheless, the cross-check using LIFULL strengthens the methodological validity of our core conclusion: spaces serving public/shared activities form the spatial core of residential floor

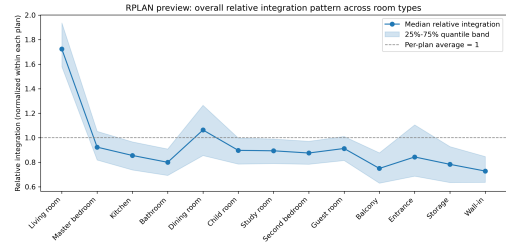
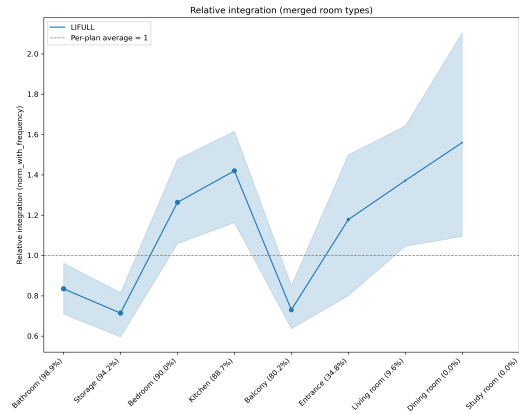
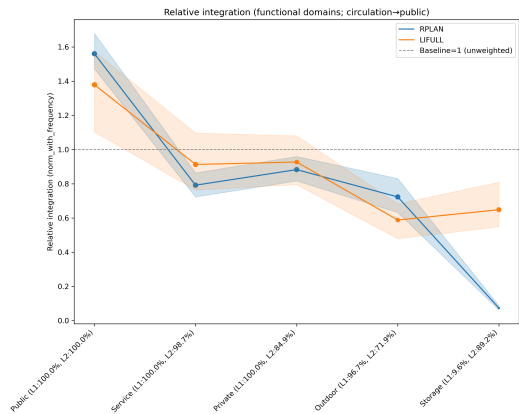


Figure 2: Overall relative integration pattern across room types



(a) Functional-domain-level harmonized comparison



(b) Cross-dataset validation of public-space dominance

Figure 3: Dataset-specific room-type coverage and labeling differences

plans, and this empirically grounded hierarchy motivates the use of living/public-space integration as a robust design prior for guiding early-stage floor plan generation.

3.2.2. Quality Evaluation of Baseline Models and Initial Model Selection

To evaluate the spatial organization of AI-generated residential floor plans against empirical architectural benchmarks, this study introduces the concept of coverage-weighted relative integration. This metric extends conventional relative integration by incorporating room-type coverage frequency, allowing integration values to reflect not only spatial

centrality but also the prevalence of each functional space across a large set of layouts. By doing so, the metric provides a more robust basis for comparing datasets with heterogeneous room-type distributions.

Fig. 4 compares the coverage-weighted relative integration profiles of the screened RPLAN dataset and 10,000 residential floor plans generated by HouseDiffusion (HD10000), one of the most stable and advanced AI-based residential floor plan generation models to date. For both datasets, integration values are normalized within each plan, and the baseline value of 1 represents the unweighted per-plan average. It should be emphasized that the HD10000 layouts are generated under constraints derived from RPLAN-based statistical priors and conditional sampling strategies. Therefore, differences between the two curves should be interpreted as degrees of fitting to and deviation from the training distribution, rather than as evidence of independent generalization across domains. The comparison thus focuses on how spatial hierarchy learned from real housing data is reproduced or distorted in AI-generated layouts.

From a single-domain perspective, a clear pattern emerges. Room types with high coverage frequencies appear at the front of the ranking and generally exhibit coverage-weighted integration values above the baseline. This indicates that these spaces tend to occupy more central positions in the majority of layouts. Room types with medium coverage frequencies cluster around the baseline, suggesting spatial centrality close to the system average. In contrast, low-coverage room types appear at the tail of the distribution and show substantially lower weighted integration values, reflecting the combined effect of rarity and peripheral spatial roles.

In terms of data reliability, room types such as living rooms, bedrooms, bathrooms, kitchens, and balconies exhibit relatively high coverage in both datasets, making their integration statistics more stable and interpretable. Conversely, room types located toward the end of the ranking—including study rooms, storage spaces, dining rooms, and entrances—have much lower coverage, and their weighted integration values should therefore be interpreted with caution. Overall, the two curves exhibit consistent global trends, indicating that HouseDiffusion successfully captures the broad spatial hierarchy present in the real-world dataset. However, notable discrepancies remain. In particular, while the living room maintains the highest coverage-weighted integration in both datasets, its degree of dominance and the gradient between subsequent room types are less well aligned with the empirical patterns observed in RPLAN. This suggests that although the generative model reproduces the overall ordering of spatial centrality, it does not yet fully replicate the strength of hierarchical differentiation characteristic of real residential layouts.

These results highlight both the effectiveness and the limitations of current AI-based residential floor plan generation models. Coverage-weighted relative integration provides a nuanced and interpretable metric for diagnosing how spatial layout knowledge derived from real housing

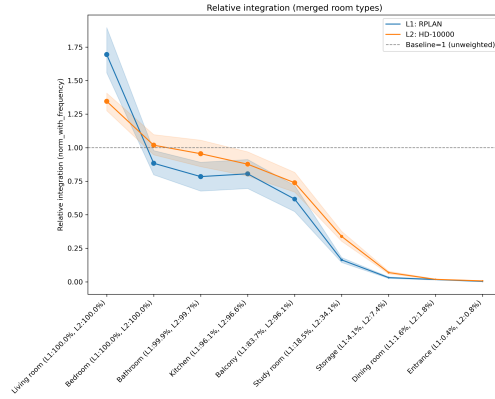


Figure 4: Comparison of Relative Integration Profiles.

data is embedded—and where it is weakened—within AI-generated designs.

3.3. Benchmark Design: Qualitative Observation and Quantitative Metrics

3.3.1. Integration-Based Screening Results on the RPLAN Dataset

The integration-based screening framework was first applied to the RPLAN dataset to assess data usability and spatial consistency prior to large-scale analysis. The original dataset contains 80,788 real residential floor plan cases, collected from real-world housing layouts and widely used in AI-based floor plan generation research. During preprocessing and topological construction, several categories of data failures were identified. These failures are not related to spatial integration computation itself but arise from upstream representation conversion and structural constraints required for automated analysis. Specifically, four types of data errors were detected (Table 2).

After excluding these invalid samples, 76,878 floor plans remained usable, corresponding to 95.16%. Importantly, the detected failures reflect practical challenges commonly encountered in large architectural datasets, such as representation inconsistencies and geometric irregularities. Without automated screening, such problematic cases could introduce noise or bias into statistical analysis and AI model evaluation. The integration-based screening framework, combined with representation-level validation, therefore plays a critical role in ensuring the reliability of downstream empirical analysis and benchmarking. The screened and validated subset of the RPLAN dataset serves as the empirical foundation for the subsequent analysis of spatial integration patterns and for comparison with AI-generated residential floor plans.

3.3.2. Custom Evaluation Metrics: Coverage-Weighted Relative Integration (CWRI)

To enable robust comparison of spatial integration patterns across large sets of residential floor plans with heterogeneous room-type distributions, this study introduces

Table 2
Summary of RPLAN dataset cleaning and usability

Step	Data Status	Meaning (Cleaning Stage)	No. Cases	Perc. (%)	Representative	Description
0.	original dataset	Raw residential floor plans collected.	80,788	100.00		Raw PNG + annotations.
1.	json_failed	PNG-to-JSON conversion failed.	3,497	4.33		Missing JSON output.
2.	build_org	Failure in original room geometry.	171	0.21		Empty room contour.
3.	build_house	Excessive room corner points.	121	0.15		Jagged boundaries.
4.	syn_skip	Samples skipped due to synthesis constraints.	121	0.15		Constraint conflict.
—	Total excluded		3,910	4.84	—	
—	Usable RPLAN	Successfully retained for analysis.	76,878	95.16		Fully computable.

Coverage-Weighted Relative Integration (CWRI) as an extension of conventional relative integration analysis. In large-scale datasets and AI-generated samples, different functional room types do not appear with equal frequency; consequently, a direct comparison based solely on average relative integration may be biased by rare room types with unstable statistics. To address this issue, CWRI incorporates room-type prevalence into the integration evaluation, ensuring that spatial roles are assessed in relation to both topological centrality and occurrence frequency.

For a given room type r , the coverage-weighted relative integration is defined as:

$$CWRI_r = \overline{RI}_r \times \omega_r, \quad (5)$$

where \overline{RI}_r denotes the mean relative integration value of room type r , computed across all floor plans in which this room type appears, and ω_r represents the coverage ratio of room type r , defined as the proportion of floor plans in the dataset that contain said room type.

Relative integration values are normalized within each floor plan such that the unweighted per-plan average equals 1. Under this normalization, a baseline value of 1 indicates average spatial centrality across all rooms within a plan. By incorporating coverage information, the proposed metric distinguishes room types that are consistently present and structurally central across most layouts from those that are infrequent and tend to occupy peripheral spatial positions. High values of $CWRI_r$ indicate room types that combine high spatial integration with widespread occurrence (“structural cores”), whereas low values reflect the combined effect

of low integration and low coverage. This formulation is particularly suitable for evaluating AI-generated residential floor plans against empirical benchmarks, as it reduces instability introduced by rare room types and allows for a meaningful comparison between real-world datasets and generated samples with varying room-type distributions.

3.3.3. Scalar Metrics: Graph Integration and Public-Space Dominance

Let a plan be represented by its rectangle-space graph $G = (V, E)$, where each node corresponds to a rectangle-based convex atom, and let s_v be the node integration score computed by the space-syntax routine. The **graph-level integration** is

$$\text{integration} = \frac{1}{|V|} \sum_{v \in V} s_v. \quad (6)$$

To measure the architectural prior that the living room should act as the configurational core, we use **public-space dominance** (public_score). Node integration is first aggregated to room-instance mean integration. For room instance r with node set V_r ,

$$\bar{s}_r = \frac{1}{|V_r|} \sum_{v \in V_r} s_v. \quad (7)$$

Let \mathcal{P} be the public-space set (by default, living room instances). Define

$$\text{public_max} = \max_{r \in \mathcal{P}} \bar{s}_r, \quad \text{other_max} = \max_{r \notin \mathcal{P}} \bar{s}_r, \quad (8)$$

then

$$\text{public_score} = \text{public_max} - \text{other_max}. \quad (9)$$

A positive `public_score` indicates that the most integrated living room dominates every non-living space in that plan.

3.3.4. Profile-Based Metrics: Relative Integration, `living_room`, and `living_adv`

Beyond scalar dominance, we also evaluate whether the generator reproduces the *hierarchical profile* of residential space observed in real data. For a merged functional category g (e.g., Living room, Bedroom, Kitchen, Bathroom, Balcony, Entrance, Storage), define category-level absolute integration for plan p :

$$I_{p,g} = \frac{\sum_{t \in g} n_{p,t} m_{p,t}}{\sum_{t \in g} n_{p,t}}. \quad (10)$$

where $n_{p,t}$ is the number of rooms of type t and $m_{p,t}$ is the mean integration of type t in plan p . We normalize within each plan to obtain a **relative integration profile**:

$$\begin{aligned} \mu_p &= \text{mean}_{g \in G_p}(I_{p,g}), \\ R_{p,g} &= \frac{I_{p,g}}{\mu_p}. \end{aligned} \quad (11)$$

where G_p is the set of valid (non-missing) merged categories in plan p used as the normalization denominator. In our analysis, the denominator category set is {Living room, Bedroom, Kitchen, Bathroom, Dining room, Study room, Balcony, Entrance, Storage} (excluding Unknown). The dataset-level curve value for category g is the median:

$$Y_g = \text{median}_p(R_{p,g}). \quad (12)$$

with $Q25_g$ and $Q75_g$ defined analogously for IQR bands.

From $R_{p,g}$ we derive two evaluation indicators that focus on the living room. For stable reporting, we define a compact visible category set $G_p^{\text{vis}} \subseteq G_p$ that excludes Entrance and Unknown; in our analysis, G_p^{vis} is {Living room, Bedroom, Kitchen, Bathroom, Dining room, Study room, Balcony, Storage}.

$$\begin{aligned} \text{living_room}_p &= R_{p,\text{Living}} \\ \text{living_adv}_p &= R_{p,\text{Living}} - \max_{g \in G_p^{\text{vis}}, g \neq \text{Living}} R_{p,g}. \end{aligned} \quad (13)$$

Intuitively, `living_room` measures how integrated the living room is relative to the plan-average integration, and `living_adv` measures how much it leads over the strongest non-living category.

Finally, to summarize profile alignment against a real-data reference (RPLAN_g in this study), we report a **median profile distance**:

$$d_{\text{profile}} = \frac{1}{|G|} \sum_{g \in G} |Y_g - Y_g^{\text{ref}}|. \quad (14)$$

where Y_g^{ref} is the reference median relative profile.

3.4. Generative Framework: Space Syntax-guided Post-training (SSPT)

Let \mathbf{c} denote the generative condition (e.g., boundary/program constraints and graph-structured semantics provided by the dataset loader), and let \mathbf{x}_0 denote the final geometric layout representation produced by the generator. In our implementation, $\mathbf{x}_0 \in \mathbb{R}^{2 \times N_v}$ represents the flattened sequence of polygon-corner coordinates. A pre-trained conditional diffusion model, denoted as $p_\theta(\mathbf{x}_0 | \mathbf{c})$, is optimized primarily for large-scale distribution fitting using standard score-matching objectives. Consequently, while it successfully captures localized geometric correlations (e.g., wall orthogonality, typical room dimensions), it may fundamentally under-emphasize the *implicit architectural priors* that are crucial for functional residential planning. Foremost among these priors is the configurational dominance of public living spaces, which governs the logical flow and human-centric usability of a dwelling.

To address this semantic gap between geometric generation and architectural configuration, we introduce **Space Syntax-guided Post-training (SSPT)**. SSPT is an advanced post-training paradigm that explicitly injects space-syntax priors into the floorplan generation process *after* the initial pre-training phase. The framework assumes access to a non-differentiable *space-syntax oracle* $\mathcal{O}(\cdot)$ that maps a generated plan to rigorous, integration-based topological measurements (as defined in Sec. 3.1–3.3). From these measurements, a scalar reward/score function $r(\cdot)$ is derived to quantify the architectural rationality of the layout.

The overarching objective of the SSPT post-training paradigm is to systematically refine the model parameters θ such that samples drawn from the generative distribution $p_\theta(\cdot | \mathbf{c})$ are statistically more likely to satisfy the target configurational logic. Mathematically, this is formulated as an expected reward maximization problem over the conditional distribution:

$$\theta^* = \arg \max_{\theta} \mathbb{E}_{\mathbf{c} \sim p(\mathbf{c}), \mathbf{x}_0 \sim p_\theta(\cdot | \mathbf{c})} [r(\mathcal{O}(\mathbf{x}_0))]. \quad (15)$$

Because the evaluation oracle \mathcal{O} encapsulates discrete, non-differentiable algorithmic steps—including rendering to RPLAN-style masks, greedy maximal-rectangle decomposition, door-component adjacency detection, graph construction, and depth-based integration computation—direct end-to-end backpropagation is mathematically intractable. Therefore, SSPT provides two practical, scalable optimization routes that remain faithful to our generative codebase: (i) **data-level refinement** via iterative filtering and retraining (SSPT-Iter), and (ii) **objective-level refinement** via reinforcement learning utilizing a clipped Proximal Policy Optimization (PPO) objective on the diffusion reverse process (SSPT-PPO).

3.4.1. The SSPT Paradigm: Knowledge-Guided Generative Refinement

The SSPT framework treats space syntax not as an implicit feature to be accidentally absorbed by a neural network, but as an explicit, computable architectural prior that supervises generation *through post-training*. This design choice prevents the degradation of pre-trained geometric stability while strictly enforcing topological rules. Concretely, the SSPT workflow is cleanly separated into two distinct operational modules:

(A) *Generative Module (Stochastic Policy Formulation)* We employ a conditional diffusion backbone as the foundational generator. Starting from a pure noise state $\mathbf{x}_T \sim \mathcal{N}(\mathbf{0}, \mathbf{I})$, the model iteratively samples a reverse denoising trajectory defined as $\mathbf{x}_T \rightarrow \mathbf{x}_{T-1} \rightarrow \dots \rightarrow \mathbf{x}_0$. Each step in this reverse transition is parameterized as a Gaussian distribution:

$$p_{\theta}(\mathbf{x}_{t-1} | \mathbf{x}_t, \mathbf{c}) = \mathcal{N}\left(\mathbf{x}_{t-1}; \boldsymbol{\mu}_{\theta}(\mathbf{x}_t, t, \mathbf{c}), \text{diag}(\boldsymbol{\sigma}_t^2)\right). \quad (16)$$

In our deep learning implementation, the transition parameters $(\boldsymbol{\mu}_{\theta}, \log \boldsymbol{\sigma}_t^2)$ are explicitly returned by the core diffusion routine `p_mean_variance`. This architectural trait is critical, as these values are utilized not only for generating geometric samples but also for computing exact log-probabilities during policy-based reinforcement learning.

(B) *Knowledge Module (The Space-Syntax Oracle)* Given the final generated layout \mathbf{x}_0 , the knowledge module serves as an automated architectural judge. The oracle renders the vectorized plan into an RPLAN-style 4-channel semantic instance mask, builds the corresponding rectangle-space graph, calculates integration scores (global HH or local closeness), and aggregates them into comprehensive plan-level and type-level statistics. These statistics, exported computationally as CSV records, include definitive metrics such as `integration` and `public_score`. Consequently, this oracle provides a highly stable, scalable, and architecture-informed supervision signal, enabling both hard data filtering (for SSPT-Iter) and continuous reward-based optimization (for SSPT-PPO).

The pivotal design choice within the SSPT paradigm is that the profound architectural prior is reliably encoded as a *measurement* rather than a differentiable proxy loss. By shifting the burden of constraint satisfaction to *post-training* procedures that handle non-differentiable rewards, SSPT guarantees compatibility with existing state-of-the-art pre-trained generators, allowing controlled, domain-specific refinement without requiring the redesign of the complex diffusion backbone.

3.4.2. Strategy I: Iterative Retraining via Space Syntactic Filtering (SSPT-Iter)

Overview of the Iterative Loop SSPT-Iter is conceived as a knowledge-guided, self-improvement loop. It operates

by repeatedly: (i) sampling a large cohort of candidate floor-plans from the current state of the generator, (ii) rigorously evaluating these candidates via the space-syntax oracle, (iii) selecting a high-quality subset that strictly adheres to the desired configurational hierarchy, and (iv) fine-tuning the diffusion model on this filtered set using the standard diffusion training objective. Because it leverages data-level curation, this strategy requires no policy gradients, making it highly robust to non-differentiable and computationally expensive architectural evaluations.

Formally, let $\mathcal{D}_{\text{base}}$ denote the high-quality real plan set (e.g., HouseGAN++ formatted JSONs) and $\mathcal{D}_{\text{gen}}^{(k)}$ denote the set of stochastically generated candidates at iteration k . SSPT-Iter constructs a refined retraining set $\mathcal{D}_{\text{top}}^{(k)}$ by executing a top- K selection mechanism over the union of both sets:

$$\mathcal{D}_{\text{top}}^{(k)} = \text{TopK}\left(\mathcal{D}_{\text{base}} \cup \mathcal{D}_{\text{gen}}^{(k)}; s(\mathbf{x}_0)\right), \quad (17)$$

where $s(\mathbf{x}_0)$ is a highly specialized integration-based score computed from the oracle’s outputs. Once the subset is curated, the diffusion model is fine-tuned by minimizing the standard denoising objective over the new distribution $\mathcal{D}_{\text{top}}^{(k)}$:

$$\min_{\theta} \mathbb{E}_{(\mathbf{x}_0, \mathbf{c}) \sim \mathcal{D}_{\text{top}}^{(k)}} \mathbb{E}_{t, \epsilon} \left[\mathcal{L}_{\text{diff}}(\theta; \mathbf{x}_0, t, \epsilon, \mathbf{c}) \right], \quad (18)$$

where $\mathcal{L}_{\text{diff}}$ represents the diffusion training loss, efficiently implemented as `training_losses` within our algorithmic codebase.

Robust Integration-Based Filtering Score The default selector for SSPT-Iter employs a *living-room dominance score*, directly aligned with the foundational architectural rule that “the living room should function as the integration core of the residence.” From the oracle-aggregated CSV reports, we extract the following for each layout: (i) the living-room mean integration μ_L (mapped as type 0 in our functional taxonomy), (ii) a collection of other room-type mean integrations $\{\mu_j\}$ representing all other functional types present in the specific plan, and (iii) foundational validity attributes such as `total_rooms`, `total_area`, and the living-room area share (ρ_L).

Given the high variance and potential for extreme structural outliers in generated spatial systems, standard z-score normalization is inadequate. Therefore, we define a robust standardized advantage term utilizing the median and the Median Absolute Deviation (MAD):

$$z(\mathbf{x}_0) = \frac{\mu_L - \text{median}(\{\mu_j\})}{\text{MAD}(\{\mu_j\}) + \epsilon}, \quad (19)$$

$$\text{MAD}(\{\mu_j\}) = \text{median}(|\mu_j - \text{median}(\{\mu_j\})|).$$

where ϵ is a small constant introduced to prevent zero-division. Within the computational pipeline, non-room and purely structural labels (e.g., exterior boundaries, walls, doors) are strictly excluded from the set $\{\mu_j\}$ via an *ignore set*. Should the MAD degenerate to zero (e.g., in overly

simplistic layouts), the scaling mechanism automatically falls back to the standard deviation.

To ensure holistic architectural rationality, we augment the dominance score with stringent, non-compensatory penalties that function as minimal plan validity gates. These penalties penalize layouts that fail fundamental habitability standards:

$$\begin{aligned} p(\mathbf{x}_0) = & \lambda_{\text{miss}} \mathbb{1}[\text{living missing}] \\ & + \lambda_{\text{rooms}} \mathbb{1}[\text{rooms} < m_{\text{min}}] \\ & + \lambda_{\text{area}} \mathbb{1}[\text{area} < a_{\text{min}}] \\ & + \lambda_{\text{share}} \mathbb{1}[\rho_L \notin [\rho_{\text{min}}, \rho_{\text{max}}]]. \end{aligned} \quad (20)$$

where ρ_L denotes the living-room area share. The final unified selection score used for the Top-K filtering is the summation:

$$s(\mathbf{x}_0) = z(\mathbf{x}_0) + p(\mathbf{x}_0). \quad (21)$$

This robust scoring function identically matches the implementation in our iterative retraining pipeline and is purposely designed to be reusable as a dense reward signal for PPO (Sec. 3.4.3), thereby guaranteeing consistent optimization targets across both post-training paradigms.

3.4.3. Strategy II: Reinforcement Learning with Space Syntactic Rewards (SSPT-PPO)

Diffusion as a Sequential Policy In contrast to offline data curation, SSPT-PPO directly and online optimizes the generator via reinforcement learning. It mathematically treats the diffusion reverse process as a finite-horizon Markov decision process (MDP). At any given timestep t , the *state* is defined as the current noisy geometric layout $\mathbf{s}_t = \mathbf{x}_t$, the *action* is the sampled denoised state for the next step $\mathbf{a}_t = \mathbf{x}_{t-1}$, and the *policy* is the localized diffusion transition modeled in Eq. (16).

To execute policy gradient updates, we compute the exact Gaussian log-probability per step. By flattening the spatial sequence over all points and x/y coordinate channels (indexed by d), the log-probability is formulated as:

$$\begin{aligned} \log \pi_{\theta}(\mathbf{a}_t | \mathbf{s}_t, \mathbf{c}) = & -\frac{1}{2} \sum_d \left(\log(2\pi) + \log \sigma_{t,d}^2 \right. \\ & \left. + \frac{(a_{t,d} - \mu_{\theta,d})^2}{\sigma_{t,d}^2} \right). \end{aligned} \quad (22)$$

where the mean vector μ_{θ} and variance vector σ_t^2 are directly retrieved from the diffusion reverse kernel.

Terminal Integration Reward Shaping Because spatial configuration cannot be assessed on intermediate noisy states, the reward is sparse and terminal. Upon completion of the full reverse trajectory, the final geometric plan \mathbf{x}_0 is passed to the space-syntax oracle, which assigns a scalar terminal reward $R = r(\mathcal{O}(\mathbf{x}_0))$. In our comprehensive implementation, this reward can be instantiated in two ways: (i) directly utilizing the robust integration-based score $s(\mathbf{x}_0)$ formulated for SSPT-Iter (Eq. (21)), ensuring parity between

methods, or (ii) constructing a hybrid, weighted-sum reward that combines multiple oracle outputs (e.g., a specific living-room term, the overall public-score term, global mean integration, and a distributional-distance penalty to a real-world reference profile), compounded with severe penalties for structural failures. To stabilize the PPO learning dynamics, these terminal rewards are subject to clipping operations, restricted either by fixed numerical bounds or by dynamic quantile ranges computed across the active rollout pool.

Clipped PPO Surrogate Update Given a dataset of on-policy rollouts sampled from the current model behavior θ_{old} , we apply a clipped Proximal Policy Optimization (PPO) objective to every individual diffusion step (excluding the final, deterministic projection step). Let the probability ratio be defined as:

$$\begin{aligned} \rho_t(\theta) = & \exp \left(\log \pi_{\theta}(\mathbf{a}_t | \mathbf{s}_t, \mathbf{c}) \right. \\ & \left. - \log \pi_{\theta_{\text{old}}}(\mathbf{a}_t | \mathbf{s}_t, \mathbf{c}) \right). \end{aligned} \quad (23)$$

and let A represent the advantage value derived from the terminal rewards. To minimize variance, we utilize a normalized terminal advantage $A = (R - \mu_R)/(\sigma_R + \epsilon)$ computed explicitly over the current rollout batch. The per-step clipped surrogate objective is subsequently defined as:

$$\mathcal{J}_t(\theta) = \min \left(\rho_t(\theta)A, \text{clip}(\rho_t(\theta), 1 - \epsilon, 1 + \epsilon)A \right). \quad (24)$$

To prevent catastrophic forgetting of the pre-trained geometric distribution, we maximize the timestep-averaged surrogate objective augmented with an explicit Kullback-Leibler (KL) divergence penalty:

$$\max_{\theta} \mathbb{E} \left[\frac{1}{T} \sum_{t=1}^T \mathcal{J}_t(\theta) - \beta_{\text{KL}} \widehat{\text{KL}}(\pi_{\theta_{\text{old}}} \| \pi_{\theta}) \right], \quad (25)$$

with the KL term estimated from stored rollouts as

$$\widehat{\text{KL}}(\pi_{\theta_{\text{old}}} \| \pi_{\theta}) = \frac{1}{T} \sum_{t=1}^T \left(\log \pi_{\theta_{\text{old}}} - \log \pi_{\theta} \right). \quad (26)$$

where the KL penalty term is efficiently estimated utilizing the actions previously sampled from the behavior policy $\pi_{\theta_{\text{old}}}$. In our main experiments, we set $\beta_{\text{KL}} = 0$ and rely on PPO clipping and a small learning rate for stability; KL regularization can be enabled if stronger anchoring to the pre-trained generator is desired. Operationally, the SSPT-PPO framework alternates dynamically between *rollout collection* (sampling complete trajectories while logging the tuple $(\mathbf{s}_t, \mathbf{a}_t, \log \pi_{\theta_{\text{old}}})$) and *policy optimization* (recalculating log-probabilities from the updating model θ and applying the gradients of Eq. (25)). This constitutes a mathematically rigorous, true on-policy post-training mechanism that directly aligns the latent steps of diffusion-based floorplan generation with high-level space-syntax priors.

Table 3

Unified SSPT-Bench (Eval-8) protocol used for all model comparisons in Sec. 4.

Component	Setting
Train-condition sampling	set_name=train, target_set=8 with room-count cap ≤ 7 (no 8-room conditions in generation during post-training).
Evaluation benchmark	set_name=eval, target_set=8 (exact 8-room constraints).
Per-checkpoint sample size	$N = 5000$ generated floorplans (robust statistics reported).
Space-syntax oracle	Rectangle-space graph integration (greedy maximal-rectangle cover); min rectangle area = 50 px; integration method hh.
Oracle outputs	Per-plan JSON reports \rightarrow aggregated convex_integration_summary.csv.
Reported statistics	mean, median, std, q25, q75, and IQR = q75 - q25.

3.5. Implementation Protocols: Model Training and Performance Assessment

3.5.1. Backbone Model and Conditioning Interface

All variations of the SSPT framework share an identical conditional diffusion backbone to ensure rigorous ablation. Layouts are represented as coordinate sequences $\mathbf{x} \in \mathbb{R}^{2 \times N}$, strictly conditioned on a semantic bundle \mathbf{c} (comprising boundary masks and adjacency graphs). This architectural isolation ensures SSPT alters only the post-training mechanics without modifying the pre-trained neural backbone.

To prevent evaluation leakage and test zero-shot configurational generalization, we enforce a strict *split-by-room-count* protocol: the generator is fine-tuned exclusively on layouts with ≤ 7 rooms and evaluated on an out-of-distribution eval-8 benchmark (layouts with exactly 8 rooms).

3.5.2. Unified Benchmark Protocol (SSPT-Bench / Eval-8)

We evaluate all models under a single **SSPT-Bench (Eval-8)** protocol, designed to measure whether the generator can satisfy space-syntax priors under an out-of-distribution (OOD) constraint regime. Specifically, both SSPT-Iter and SSPT-PPO are trained using *train-condition sampling* capped at ≤ 7 rooms (to avoid sampling 8-room conditions during post-training), while evaluation is conducted on the *Eval-8* benchmark that contains exactly 8 rooms. All scalar metrics and profile curves are computed from the same oracle outputs (per-plan reports aggregated to a summary CSV) and analyzed by a unified evaluation pipeline to ensure reproducibility.

3.5.3. Space Syntax Oracle: Rectangle-based Integration Pipeline

Given a generated layout \mathbf{x}_0 , the non-differentiable architectural oracle executes a deterministic four-stage pipeline:

1. **Rendering & Rasterization:** Polygon-vertex sequences are decoded into standardized RPLAN-style 4-channel semantic instance masks (ch1/ch2/ch3/ch4).
2. **Rectangle Decomposition:** For each room instance, the walkable core mask is decomposed into maximal axis-aligned rectangles via greedy covering, controlled by a minimum rectangle area threshold.
3. **Graph Construction & Integration Computation:** A rectangle-space graph is constructed using same-room proximity edges and interior-door-mediated cross-room edges. Node-specific integration scores

are then computed (HH or closeness) and aggregated (via room-instance averaging) into plan-level scalars such as `public_score`.

4. **Data Aggregation:** Granular metrics are compiled into a unified CSV ledger, ensuring metric integrity across dataset screening, reward formulation, and final evaluation.

3.5.4. Post-Training Optimization Protocols

We implement two distinct optimization routes based on the oracle’s output:

SSPT-Iter (Automated Filtering and Fine-tuning): Operating offline, this protocol samples a batch of N layouts under the ≤ 7 room condition, processes them through the oracle, and applies the robust advantage score $s(\mathbf{x}_0)$ (Eq. 21). The Top- K subset is materialized to dynamically override the training data, allowing the model to fine-tune its parameters using the standard L_2 denoising objective.

SSPT-PPO (On-policy Rollouts and Optimization): Operating online, this protocol collects full reverse-diffusion trajectories from pure noise $\mathbf{x}_T \sim \mathcal{N}(0, I)$, logging state-action-probability tuples for all timesteps. The terminal layout \mathbf{x}_0 is evaluated by the oracle to assign a quantile-clipped terminal reward. The model subsequently recalculates step-wise log-probabilities and updates the policy via the clipped PPO objective (Eq. 25) over multiple sub-epochs.

3.5.5. Performance Assessment and Reporting

Model efficacy is evaluated on the eval-8 benchmark. Given the heavy-tailed nature of graph-based integration metrics, we report robust central tendencies (median and interquartile range) alongside standard deviations. The syntactic fidelity is quantified via three primary integration-derived indicators:

1. **Public-space Dominance (`public_score`):** The numerical difference between the maximum mean integration of designated public spaces (e.g., living rooms) and the highest mean integration among all subordinate private/service rooms.
2. **Relative Living-room Integration (`living_room`):** The living-room’s absolute integration normalized by the within-plan integration average across all functional categories (baseline = 1).
3. **Living-room Advantage (`living_adv`):** The relative integration margin of the living room over the next

most integrated non-living functional space within the same layout.

These scalars are complemented by a distributional comparative analysis of room-type integration profiles, directly mapping generated samples against the screened real-world data reference.

4. Results

4.1. Evaluation System Restatement and Unified Benchmark

This section briefly restates the evaluation system and reports results under a single unified benchmark protocol so that the design, implementation, and reported results are fully consistent. All models are evaluated on **SSPT-Bench (Eval-8)** (Table 3), and all evaluation metrics are computed by the same space-syntax oracle described in Sec. 3.5.

We report robust statistics (median, std, and IQR) of three primary indicators—public-space dominance (public_score , Eq. (9)), living-room relative integration (living_room , Eq. (13)), and living-room advantage (living_adv , Eq. (13))—as well as the room-type profile distance to the real-data reference (d_{profile} , Eq. (14)). Unless otherwise stated, statistics are computed over $N = 5000$ generated plans per checkpoint; RPLAN₈ is used as the real-data reference.

4.2. Evaluation System Applied to Model Performance Analysis

We compare two post-training paradigms under SSPT-Bench: **SSPT-Iter** (iterative retraining with space-syntax filtering and diffusion fine-tuning) and **SSPT-PPO** (on-policy PPO alignment with space-syntax rewards). For fairness, both paradigms start from the same pretrained HouseDiffusion baseline checkpoint and are evaluated on the same Eval-8 protocol with $N = 5000$ generated samples per checkpoint. We report the baseline generator as **HD5000** and the real-data reference as **RPLAN₈**.

4.2.1. Effect Comparison: SSPT-Iter vs SSPT-PPO (Qualitative and Quantitative)

Table 4 summarizes the main scalar metrics on Eval-8 for HD5000, SSPT-Iter (Iter5), SSPT-PPO (PPO10), and the real reference RPLAN₈. The key quantitative findings are:

- Stronger public-space dominance under PPO:** SSPT-PPO improves the median public_score from 0.1820 (SSPT-Iter) to 0.2244 (+0.0424), and simultaneously reduces dispersion (std/IQR) by roughly 20%–24%.
- More reliable living-room advantage:** SSPT-PPO improves the median living_adv from 0.3149 to 0.3522 (+0.0374), also with reduced dispersion (std/IQR \approx 22% reduction).
- Comparable living-room level but much higher stability:** The median living_room is essentially unchanged (1.4195 \rightarrow 1.4169, -0.0026), but SSPT-PPO significantly narrows the distribution (std/IQR

\approx 31% reduction), indicating that PPO makes the generation outcome more controllable and less sensitive to stochastic sampling.

In addition to scalar metrics, we evaluate cross-category configurational alignment using the median relative integration profile distance in Eq. (14). SSPT-PPO achieves substantially better profile alignment to RPLAN₈: $d_{\text{profile}} = 0.1131$ (**HD5000**) \rightarrow 0.0912 (**SSPT-Iter**) \rightarrow 0.0663 (**SSPT-PPO**). This corresponds to a 19.3% reduction from HD5000 to SSPT-Iter and a 41.3% reduction from HD5000 to SSPT-PPO, showing that PPO improves not only one or two headline scalars but also the overall functional hierarchy profile across room categories.

4.2.2. Efficiency Comparison: SSPT-Iter vs SSPT-PPO (Qualitative and Quantitative)

SSPT-Iter improves architectural alignment by repeatedly generating candidates, computing oracle metrics, filtering top- K samples, and performing diffusion fine-tuning on the rebuilt dataset. This full retraining loop is computationally heavy because each iteration includes substantial supervised diffusion training. By contrast, SSPT-PPO performs policy optimization directly on stored on-policy rollouts, and the expensive oracle step (convex integration) is executed once per rollout batch to build terminal rewards; the subsequent PPO updates operate purely in model space.

In our experiments (same hardware setting), the end-to-end wall-clock time per post-training iteration is: **8.30 hours/iter** for SSPT-Iter versus **0.75 hours/iter** for SSPT-PPO, yielding an **11.1 \times** per-iteration speedup. Furthermore, when normalized by achieved improvement on the headline metric public_score , SSPT-PPO exhibits roughly an order-of-magnitude higher gain rate.

PPO timestep respacing and practical efficiency. A key implementation factor behind SSPT-PPO’s efficiency is the diffusion-horizon setting used during rollout and optimization. PPO requires storing per-step latent states/actions and log-probabilities along the reverse-diffusion trajectory; therefore, the memory footprint and optimization cost scale approximately linearly with the number of sampled timesteps. In early trials, we attempted PPO fine-tuning using a long horizon (roughly half of the base diffusion process), which severely constrained the feasible batch size and reduced throughput, resulting in slow training and only modest metric gains.

We found that integration-based space-syntax rewards are most sensitive to the low-noise denoising region that directly determines final room geometry and accessibility relations. Consequently, in our main configuration we employ a short respaced policy of 100 steps while retaining a 1000-step base diffusion schedule, using $\text{timestep_respacing} = 80, 20, 0, 0$. This allocates most optimization steps to the late-stage denoising portion (and discards the high-noise half), enabling substantially larger rollout parallelism and yielding fast, stable improvements consistent with the effect and efficiency results reported in Tables 4 and 5.

Table 4

SSPT-Bench (Eval-8) scalar metric comparison. Reported statistics are computed over $N = 5000$ generated plans per model checkpoint; RPLAN₈ is the real-data reference ($N = 20348$).

Metric	HD5000 _{med}	SSPT-Iter _{med} (Iter5)	SSPT-PPO _{med} (PPO10)	RPLAN _{8,med}	SSPT-Iter _σ	SSPT-PPO _σ	SSPT-Iter _{IQR}	SSPT-PPO _{IQR}
public_score	0.1292	0.1820	0.2244	0.5226	0.1871	0.1425	0.2220	0.1769
living_adv	0.2413	0.3149	0.3522	0.6172	0.2101	0.1627	0.2557	0.1983
living_room	1.3397	1.4195	1.4169	1.6286	0.1725	0.1189	0.1704	0.1170

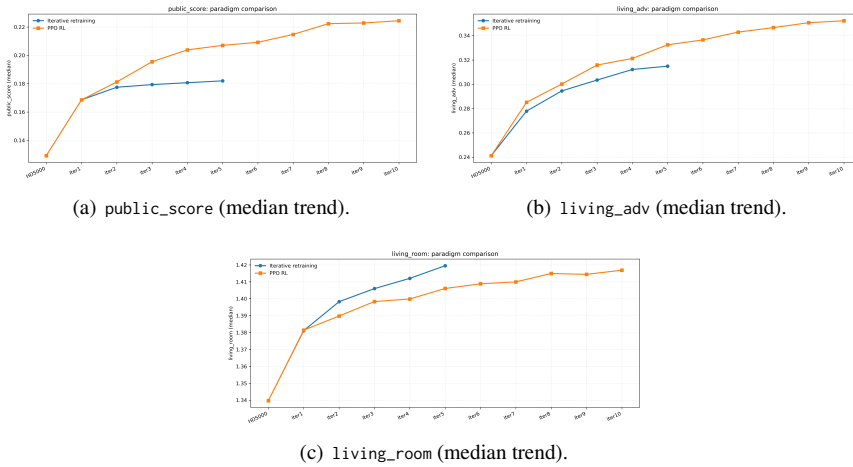


Figure 5: SSPT-Bench (Eval-8) median trends over post-training iterations. SSPT-PPO consistently improves public-space dominance and living-room advantage, while producing a notably narrower (more stable) distribution for living-room relative integration.

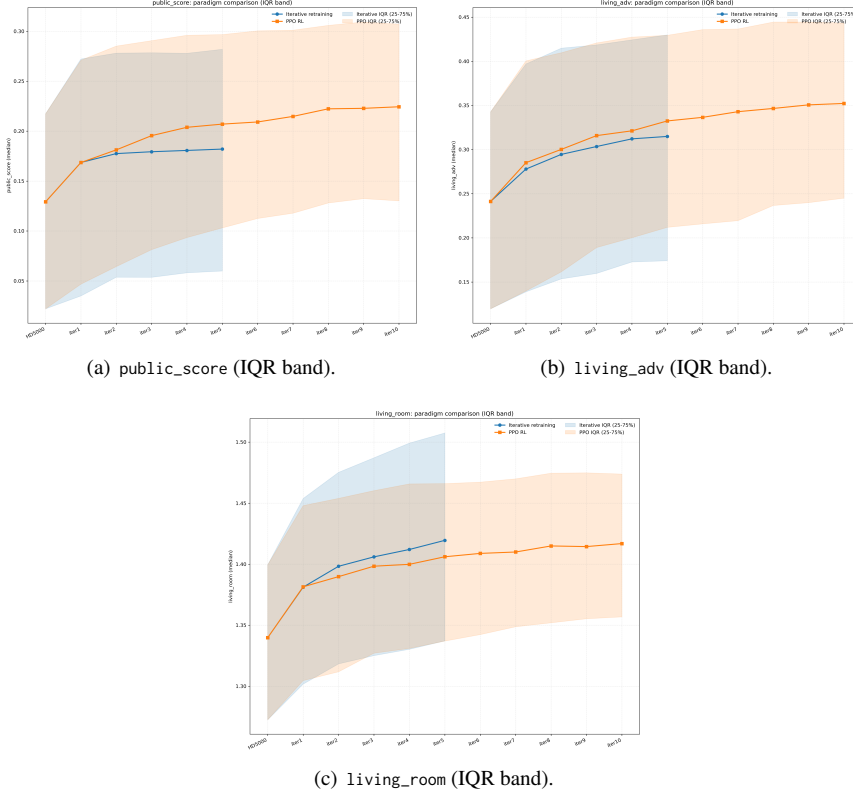


Figure 6: Robust dispersion comparison under SSPT-Bench (Eval-8). IQR bands show that SSPT-PPO yields not only higher medians on public_score and living_adv, but also consistently tighter distributions, indicating improved controllability and reduced sensitivity to sampling noise.

Table 5

Efficiency comparison (measured end-to-end per iteration in our runs). The last column reports indicative improvement rate on `public_score` relative to HD5000.

Paradigm	Time/iter (h)	Iterations to checkpoint	Total time (h)	$\Delta\text{public_score}/h$
SSPT-Iter (Iter5)	8.30	5	41.5	$\frac{0.1820-0.1292}{41.5} = 0.00127$
SSPT-PPO (PPO10)	0.75	10	7.5	$\frac{0.2244-0.1292}{7.5} = 0.01269$

Overall, SSPT-PPO provides a substantially more compute efficient post-training mechanism: it achieves higher public-space dominance and living-room advantage while also reducing metric variance, which in practice reduces the sampling budget required to obtain high-quality candidates.

4.3. Evaluation System Applied to Case Analysis

We now apply the evaluation system to interpret *what* configurational issues are corrected by SSPT post-training. Rather than relying on subjective visual inspection, we diagnose changes through the room-type relative integration profile and the living-room dominance indicators.

4.3.1. Case A: Over-centralized Threshold Spaces (Entrance)

A common configurational failure mode in purely distribution fitted generators is that threshold or circulation spaces become excessively integrated, weakening the intended public-private hierarchy. Under SSPT-Bench, this manifests as an elevated relative integration for Entrance. The RPLAN_8 reference median Entrance relative integration is 0.8246, while HD5000 yields 1.0083, suggesting an over-centralized entrance. SSPT-Iter reduces this to 0.9110, and SSPT-PPO further reduces it to 0.8766, moving closer to the empirical reference.

4.3.2. Case B: Over-integrated Private/Service Rooms (Bedroom and Bathroom)

HD5000 exhibits a flattened hierarchy in which private/service rooms are too integrated compared to RPLAN_8 (e.g., Bedroom: 1.0168 vs 0.9208; Bathroom: 0.9563 vs 0.7899). SSPT-PPO reduces Bedroom to 0.9545 and Bathroom to 0.9001, indicating stronger segregation of private/service spaces and a clearer functional hierarchy. This correction contributes directly to improved `public_score` and `living_adv`.

4.3.3. Case C: Public-Core Consistency (High `living_adv` with Low Variance)

Although both post-trained models remain below the RPLAN_8 reference in absolute living-room relative integration (Living room: 1.4195 for SSPT-Iter and 1.4169 for SSPT-PPO versus 1.6286 in RPLAN_8), SSPT-PPO achieves higher public dominance and advantage by suppressing competing maxima in non-living categories. Importantly, SSPT-PPO yields much lower dispersion on `living_room` (IQR 0.1170 vs 0.1704), meaning the public-core pattern is realized more consistently across generated plans.

In summary, the case analysis demonstrates that SSPT post-training primarily improves floorplan generation by **strengthening the public-space dominance rule and restoring a clearer functional hierarchy** across room categories, and SSPT-PPO achieves these improvements with **higher stability and substantially higher compute efficiency** than iterative retraining.

5. Conclusion and Future Work

This paper proposed **Space Syntax-guided Post-training (SSPT)** to address a key limitation of distribution-fitted floor plan generators: important architectural priors can be under-emphasized when optimization is dominated by large-scale likelihood fitting. SSPT introduces a non-differentiable, space-syntax oracle that converts RPLAN-style layouts into a rectangle-space graph and computes integration-based measurements, enabling explicit post-training supervision for configurational objectives. To make the evaluation reproducible and comparable across paradigms, we further introduced **SSPT-Bench (Eval-8)**, an out-of-distribution benchmark that post-trains models under ≤ 7 -room conditions while evaluating on 8-room programs with a unified metric suite.

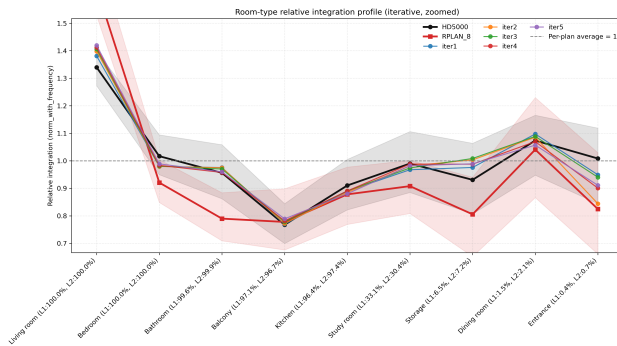
Under SSPT-Bench, both post-training strategies improve public-space dominance and functional hierarchy compared with the pretrained baseline. In particular, **SSPT-PPO** achieves stronger gains on dominance-related indicators (e.g., `public_score` and `living_adv`) while substantially reducing variance and improving overall profile alignment, and it does so with an order-of-magnitude higher practical efficiency than iterative retraining. These results suggest that post-training provides a practical and extensible pathway to integrate architectural theory into generative design, as long as a reliable post-hoc oracle is available.

Future work. Several directions can further extend SSPT. First, beyond integration dominance, future benchmarks and reward designs can incorporate a richer set of space-syntax and architectural criteria (e.g., circulation efficiency, choice/control measures, public-private zoning consistency), and explore multi-objective post-training under different constraints. Second, the current oracle relies on deterministic mask parsing, greedy rectangle decomposition, and graph computation; accelerating this pipeline (or learning faithful surrogate evaluators) would enable larger-scale post-training and more diverse reward shaping. Third, while we instantiate SSPT on a diffusion backbone, the framework can

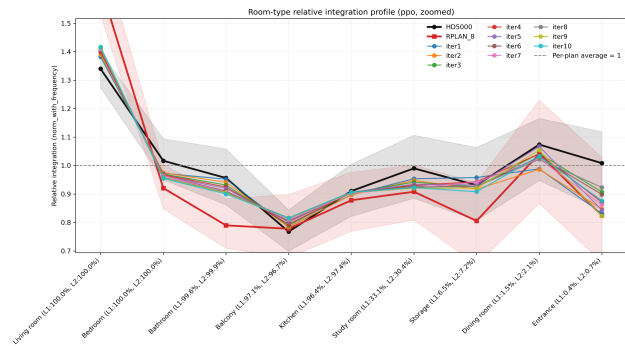
Table 6

Room-type median relative integration (selected categories). Values are medians of $R_{p,g}$ in Eq. (11); smaller deviations to $RPLAN_8$ indicate better hierarchy alignment.

Category (median Y_g)	HD5000	SSPT-Iter (Iter5)	SSPT-PPO (PPO10)	RPLAN ₈
Living room	1.3397	1.4195	1.4169	1.6286
Bedroom	1.0168	0.9889	0.9545	0.9208
Bathroom	0.9563	0.9599	0.9001	0.7899
Entrance	1.0083	0.9110	0.8766	0.8246
Storage	0.9309	0.9890	0.9081	0.8056



(a) SSPT-Iter: median relative profiles across iterations (zoomed).



(b) SSPT-PPO: median relative profiles across iterations (zoomed).

Figure 7: Room-type relative integration profile evolution under SSPT-Bench. SSPT-PPO yields a closer overall match to the empirical hierarchy in $RPLAN_8$, particularly by reducing over-integration of non-public categories (e.g., Entrance/Bedroom/Bathroom), which increases living-room dominance and advantage without requiring a large increase in the absolute living-room level.

be applied to other generators (e.g., transformer- or graph-based models) by treating the generator as a conditional sampling policy and reusing the same oracle-defined supervision. Finally, integrating SSPT with human-in-the-loop design feedback and downstream engineering constraints (e.g., structural feasibility and code compliance) remains an important step toward deployable AI-assisted residential layout design.

References

- [1] Aalaei, M., Saadi, M., Rahbar, M., Ekhlassi, A., 2023. Architectural layout generation using a graph-constrained conditional generative adversarial network (gan). *Automation in Construction* 155, 105053.
- [2] Askarizad, R., Lamíquíz Daudén, P.J., Garau, C., 2024. The application of space syntax to enhance sociability in public urban spaces: A systematic review. *ISPRS International Journal of Geo-Information* 13. URL: <https://www.mdpi.com/2220-9964/13/7/227>, doi:10.3390/ijgi13070227.
- [3] Basu, S., Kumar, A., Seshadhri, C., 2021. The complexity of testing all properties of planar graphs, and the role of isomorphism. *ArXiv abs/2108.10547*. URL: <https://api.semanticscholar.org/CorpusID:237278741>.
- [4] Can, I., Heath, T., 2016. In-between spaces and social interaction: a morphological analysis of izmir using space syntax. *Journal of Housing and the Built Environment* 31, 31–49. URL: <https://api.semanticscholar.org/CorpusID:55678336>.
- [5] Carmona, M., 2018. Principles for public space design, planning to do better. *URBAN DESIGN International* 24, 47–59. URL: <https://api.semanticscholar.org/CorpusID:115439896>.
- [6] Christiano, P.F., Leike, J., Brown, T., Martic, M., Legg, S., Amodei, D., 2017. Deep reinforcement learning from human preferences. *Advances in neural information processing systems* 30.
- [7] Credo, A., Fabri, G., Villani, M., Popescu, M., 2020. Adopting the topology optimization in the design of high-speed synchronous reluctance motors for electric vehicles. *IEEE Transactions on Industry Applications* 56, 5429–5438. doi:10.1109/TIA.2020.3007366.
- [8] Cruz, S., Hutchcroft, W., Li, Y., Khosravan, N., Boyadzhiiev, I., Kang, S.B., 2021. Zillow indoor dataset: Annotated floor plans with 360deg panoramas and 3d room layouts, in: *Proceedings of the IEEE/CVF conference on computer vision and pattern recognition*, pp. 2133–2143.
- [9] Deitke, M., VanderBilt, E., Herrasti, A., Weihs, L., Salvador, J., Ehsani, K., Han, W., Kolve, E., Farhadi, A., Kembhavi, A., et al., 2022. Proctor: Large-scale embodied ai using procedural generation. *arXiv e-prints*, arXiv-2206.
- [10] Edgü, E., Ünlü, A., 2003. Relation of domestic space preferences with space syntax parameters. URL: <https://api.semanticscholar.org/CorpusID:146403316>.
- [11] Eloy, S., Guerreiro, R., 2016. Transforming housing typologies. *space syntax evaluation and shape grammar generation*. *arq.urb*, 86–114.
- [12] Fan, Y., Watkins, O., Du, Y., Liu, H., Ryu, M., Boutilier, C., Abbeel, P., Ghavamzadeh, M., Lee, K., Lee, K., 2023. Dpok: Reinforcement learning for fine-tuning text-to-image diffusion models. *Advances in Neural Information Processing Systems* 36, 79858–79885.
- [13] Hansen, N., Ostermeier, A., 2001. Completely derandomized self-adaptation in evolution strategies. *Evolutionary computation* 9, 159–195.
- [14] Hanson, J., 1999. *Contents*. Cambridge University Press. p. v–v.
- [15] He, F., Huang, Y., Wang, H., 2022. iplan: Interactive and procedural layout planning, in: *Proceedings of the IEEE/CVF Conference on Computer Vision and Pattern Recognition*, pp. 7793–7802.

- [16] Helme, L., Derix, C., Izaki, Å., 2014. Spatial configuration: Semi-automatic methods for layout generation in practice. *The Journal of Space Syntax* 5, 35–49. URL: <https://api.semanticscholar.org/CorpusID:59127252>.
- [17] Hillier, B., 1996. Space is the machine: A configurational theory of architecture. URL: <https://api.semanticscholar.org/CorpusID:60919128>.
- [18] Hu, R., Huang, Z., Tang, Y., Van Kaick, O., Zhang, H., Huang, H., 2020. Graph2plan: Learning floorplan generation from layout graphs. *ACM Transactions on Graphics (TOG)* 39, 118–1.
- [19] Hu, S., Wu, W., Wang, Y., Xu, B., Zheng, L., 2024. Advancing architectural floorplan design with geometry-enhanced graph diffusion. *arXiv preprint arXiv:2408.16258* 8.
- [20] Jiang, B., Claramunt, C., Klarqvist, B., 2000. Integration of space syntax into gis for modelling urban spaces. *International Journal of Applied Earth Observation and Geoinformation* 2, 161–171. URL: <https://www.sciencedirect.com/science/article/pii/S0303243400850102>, doi:[https://doi.org/10.1016/S0303-2434\(00\)85010-2](https://doi.org/10.1016/S0303-2434(00)85010-2).
- [21] Kalervo, A., Ylioinas, J., Häikiö, M., Karhu, A., Kannala, J., 2019. Cubicasa5k: A dataset and an improved multi-task model for floorplan image analysis, in: *Scandinavian Conference on Image Analysis*, Springer. pp. 28–40.
- [22] Kiyota, Y., 2018. Promoting open innovations in real estate tech: Provision of the lifull home’s data set and collaborative studies, in: *Proceedings of the 2018 ACM on International Conference on Multimedia Retrieval*, pp. 6–6.
- [23] Liu, J., Xue, Y., Duarte, J., Shekhawat, K., Zhou, Z., Huang, X., 2022. End-to-end graph-constrained vectorized floorplan generation with panoptic refinement, in: *European Conference on Computer Vision*, Springer. pp. 547–562.
- [24] Luo, Z., Huang, W., 2022. Floorplan: Vector residential floorplan adversarial generation. *Automation in construction* 142, 104470.
- [25] Luo, Z.H., Lara, L., Luo, G.Y., Golemo, F., Beckham, C., Pal, C., 2024. Dstruct2design: Data and benchmarks for data structure driven generative floor plan design. *arXiv preprint arXiv:2407.15723* .
- [26] Mehrinejad Khotbehsara, E., Yu, R., Somasundaraswaran, K., Askarizad, R., Kolbe-Alexander, T., 2025. The walkable environment: a systematic review through the lens of space syntax as an integrated approach. *Smart and Sustainable Built Environment* doi:10.1108/SASBE-02-2024-0049.
- [27] Mirza, M., Osinderó, S., 2014. Conditional generative adversarial nets. *arXiv preprint arXiv:1411.1784* .
- [28] Mouret, J.B., Clune, J., 2015. Illuminating search spaces by mapping elites. *arXiv preprint arXiv:1504.04909* .
- [29] Nauata, N., Chang, K.H., Cheng, C.Y., Mori, G., Furukawa, Y., 2020. House-gan: Relational generative adversarial networks for graph-constrained house layout generation, in: *Computer Vision – ECCV 2020: 16th European Conference, Glasgow, UK, August 23–28, 2020, Proceedings, Part I*, Springer-Verlag, Berlin, Heidelberg. p. 162–177. URL: https://doi.org/10.1007/978-3-030-58452-8_10, doi:10.1007/978-3-030-58452-8_10.
- [30] Nauata, N., Hosseini, S., Chang, K.H., Chu, H., Cheng, C.Y., Furukawa, Y., 2021. House-gan++: Generative adversarial layout refinement network towards intelligent computational agent for professional architects, in: *Proceedings of the IEEE/CVF conference on computer vision and pattern recognition*, pp. 13632–13641.
- [31] Ouyang, L., Wu, J., Jiang, X., Almeida, D., Wainwright, C., Mishkin, P., Zhang, C., Agarwal, S., Slama, K., Ray, A., et al., 2022. Training language models to follow instructions with human feedback. *Advances in neural information processing systems* 35, 27730–27744.
- [32] Para, W., Guerrero, P., Kelly, T., Guibas, L.J., Wonka, P., 2021. Generative layout modeling using constraint graphs, in: *Proceedings of the IEEE/CVF International Conference on Computer Vision (ICCV)*, pp. 6690–6700.
- [33] Rafailov, R., Sharma, A., Mitchell, E., Manning, C.D., Ermon, S., Finn, C., 2023. Direct preference optimization: Your language model is secretly a reward model. *Advances in neural information processing systems* 36, 53728–53741.
- [34] Rechavi, T.B., 2009. A room for living: Private and public aspects in the experience of the living room. *Journal of Environmental Psychology* 29, 133–143. URL: <https://www.sciencedirect.com/science/article/pii/S027249440800042X>, doi:<https://doi.org/10.1016/j.jenvp.2008.05.001>.
- [35] Regenwetter, L., Nobari, A.H., Ahmed, F., 2021. Deep generative models in engineering design: A review. *CoRR abs/2110.10863*. URL: <https://arxiv.org/abs/2110.10863>, arXiv:2110.10863.
- [36] Ren, A.Z., Lidard, J., Ankile, L.L., Simeonov, A., Agrawal, P., Majumdar, A., Burchfiel, B., Dai, H., Simchowit, M., 2024. Diffusion policy optimization. *arXiv preprint arXiv:2409.00588* .
- [37] Ross, S., Gordon, G., Bagnell, D., 2011. A reduction of imitation learning and structured prediction to no-regret online learning, in: *Proceedings of the fourteenth international conference on artificial intelligence and statistics, JMLR Workshop and Conference Proceedings*. pp. 627–635.
- [38] Schulman, J., Wolski, F., Dhariwal, P., Radford, A., Klimov, O., 2017. Proximal policy optimization algorithms. *arXiv preprint arXiv:1707.06347* .
- [39] Shabani, M.A., Hosseini, S., Furukawa, Y., 2023. Housediffusion: Vector floorplan generation via a diffusion model with discrete and continuous denoising, in: *Proceedings of the IEEE/CVF conference on computer vision and pattern recognition*, pp. 5466–5475.
- [40] Singh, A., Co-Reyes, J.D., Agarwal, R., Anand, A., Patil, P., Garcia, X., Liu, P.J., Harrison, J., Lee, J., Xu, K., et al., 2023. Beyond human data: Scaling self-training for problem-solving with language models. *arXiv preprint arXiv:2312.06585* .
- [41] Sun, J., Wu, W., Liu, L., Min, W., Zhang, G., Zheng, L., 2022. Wallplan: synthesizing floorplans by learning to generate wall graphs. *ACM Transactions on Graphics (TOG)* 41, 1–14.
- [42] Tang, H., Zhang, Z., Shi, H., Li, B., Shao, L., Sebe, N., Timofte, R., Van Gool, L., 2023. Graph transformer gans for graph-constrained house generation, in: *Proceedings of the IEEE/CVF Conference on Computer Vision and Pattern Recognition*, pp. 2173–2182.
- [43] Upadhyay, A., Dubey, A., Arora, V., Kuriakose, S.M., Agarwal, S., 2022. Flnet: graph constrained floor layout generation, in: *2022 IEEE International Conference on Multimedia and Expo Workshops (ICMEW)*, IEEE. pp. 1–6.
- [44] Vignali, V., Acerra, E.M., Lantieri, C., Di Vincenzo, F., Piacentini, G., Pancaldi, S., 2021. Building information modelling (bim) application for an existing road infrastructure. *Automation in Construction* 128, 103752. URL: <https://www.sciencedirect.com/science/article/pii/S092658052100203X>, doi:<https://doi.org/10.1016/j.autcon.2021.103752>.
- [45] Wang, Y., Kordi, Y., Mishra, S., Liu, A., Smith, N.A., Khoshabi, D., Hajishirzi, H., 2023. Self-instruct: Aligning language models with self-generated instructions, in: *Proceedings of the 61st annual meeting of the association for computational linguistics (volume 1: long papers)*, pp. 13484–13508.
- [46] Wu, W., Fu, X.M., Tang, R., Wang, Y., Qi, Y.H., Liu, L., 2019. Data-driven interior plan generation for residential buildings. *ACM Trans. Graph.* 38. URL: <https://doi.org/10.1145/3355089.3356556>, doi:10.1145/3355089.3356556.
- [47] Zhan, F., Yu, Y., Wu, R., Zhang, J., Lu, S., Liu, L., Kortylewski, A., Theobalt, C., Xing, E., 2023. Multimodal image synthesis and editing: The generative ai era. URL: <https://arxiv.org/abs/2112.13592>, arXiv:2112.13592.
- [48] Zhang, L., Rao, A., Agrawala, M., 2023. Adding conditional control to text-to-image diffusion models, in: *Proceedings of the IEEE/CVF international conference on computer vision*, pp. 3836–3847.
- [49] Zhao, H., Chen, H., Zhang, J., Yao, D.D., Tang, W., 2024. Scores as actions: a framework of fine-tuning diffusion models by continuous-time reinforcement learning. *arXiv preprint arXiv:2409.08400* .
- [50] Zheng, J., Zhang, J., Li, J., Tang, R., Gao, S., Zhou, Z., 2020. Structured3d: A large photo-realistic dataset for structured 3d modeling, in: *European Conference on Computer Vision*, Springer. pp. 519–535.

- [51] Zheng, Z., Petzold, F., 2023. Neural-guided room layout generation with bubble diagram constraints. *Automation in construction* 154, 104962.